Localized electronic states in coupled superlattices

Maria Stęślicka and Robert Kucharczyk
Institute of Experimental Physics, University of Wrocław, pl. Borna 9, 50-204 Wrocław, Poland
(Received 2 August 1996)

Theoretical investigation of the electronic structure of GaAs/AlAs superlattices coupled via an $Al_yGa_{1-y}As$ spacer layer is presented. A direct matching procedure within an envelope-function approximation is used to derive the expressions for the energy and the corresponding wave function of localized electronic states appearing inside the minigaps. The transformation from a Tamm-like interface state to an above-barrier localized state is discussed. The density-of-states distributions inside the minibands are computed using the factorization and direct Green function methods. A possibility of the existence of a well-defined interface resonance in the lowest miniband is shown. [S0163-1829(97)01203-4]

INTRODUCTION

In recent years, there is a growing interest in studying the effect of a carrier localization in the so-called coupled superlattices (SL's), i.e., two SL's separated by a spacer-barrier layer.[1–8] A proper design of SL's and the spacer-layer parameters leads to quantum states with eigenfunctions mostly confined to the spacer region. Such a combined SL structure has been used to show the possibility of localizing the carrier wave function to a quantum barrier.[1] These so-called above-barrier localized states, recently observed experimentally by photoluminescence,[2] resonant Raman scattering,[5,6] as well as magnetooptical spectroscopy,[8] are very interesting for at least two reasons. One is of a general nature, as the localization of an electron in a quantum barrier is in itself a different quantum-mechanical effect. The other one concerns the possible applications: if electrons are confined long enough to recombine, a possibility of radiative transitions appears in the spacer-barrier region, leading to a luminescence at shorter wavelength than that available by similar devices. On the other hand, Tamm surface states, i.e., electronic states localized mostly in the outermost SL quantum well, have been investigated theoretically and observed experimentally in SL's (for a review see, e.g., Refs. 9 and 10). Similar surface-localized states, called then interface states, have also been considered in coupled SL's.[3,4]

The aim of this work is to study the properties of localized electronic states appearing in coupled SL's, and, in particular, their transformation from a Tamm-like interface state to an above-barrier localized state—a problem that has not been considered in any of the above-mentioned papers. Moreover, as it is known, the occurence of localized states inside the SL minigaps affects also the distribution of extended states forming the SL minibands. Therefore, we present here the density-of-states as well as the space-charge distributions calculations for a system of coupled SL's.

MODEL

We restrict our considerations to a special class of coupled SL's, namely, to a system of two identical semi-infinite SL's with fixed parameters and made of GaAs and AlAs layers, and being coupled via a spacer layer of $Al_yGa_{1-y}As$. Characteristic parameters of the structure are defined in Fig. 1. Obviously, the potential V_s of the spacer-barrier layer is always lower than that of the SL barriers V_b.

METHOD OF CALCULATION

Following our previous work,[11] we have used the direct matching procedure within the envelope-function approximation to obtain the energy expression and the corresponding wave functions for localized electronic states appearing inside the SL minigaps. First, using Bastard's boundary conditions and the Bloch requirement the wave function $\Psi_{sl}(z)$ for the right-hand-side SL has been constructed, which, for the first SL well layer $(0<z<a)$, takes the form[11]

$$\Psi_{sl}(z)=A_1[\sin(k_a z)+\lambda\cos(k_a z)], \tag{1}$$

with A_1 being a constant and

$$\lambda=\frac{\sin(k_a a)+(-1)^n K\sinh(k_b b)\exp(-\mu d)}{(-1)^n\cosh(k_b b)\exp(-\mu d)-\cos(k_a a)}. \tag{2}$$

In Eqs. (1) and (2), $K=(k_a m_b)/(k_b m_a)$, $k_a=(2m_a E)^{1/2}$, $k_b=[2m_b(V_b-E)]^{1/2}$, $d=a+b$ is the period of the SL, and

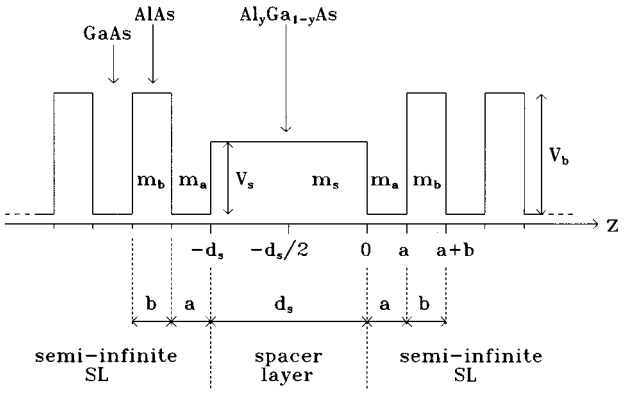

FIG. 1. Potential profile of the structure under consideration. Semi-infinite SL's are composed of GaAs wells of width a and AlAs barriers of width b and height V_b, while the $Al_yGa_{1-y}As$ spacer-barrier layer is of thickness d_s and height V_s. Effective masses in the corresponding layers are denoted by m_a, m_b, and m_s.

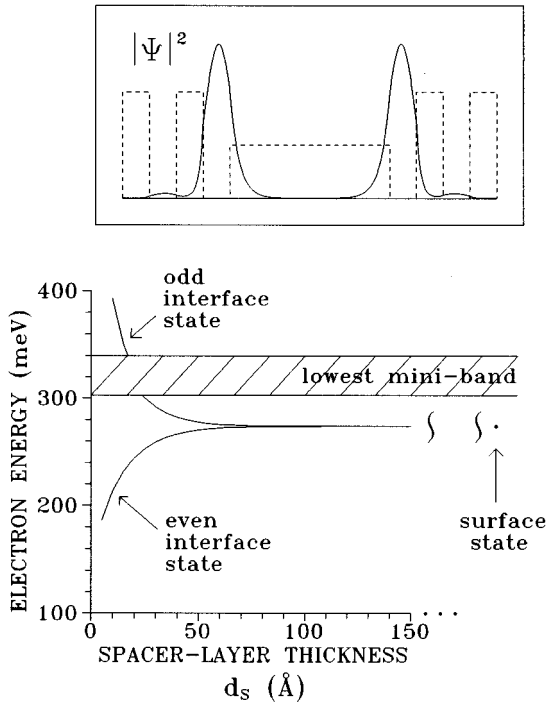

FIG. 2. Electronic structure of GaAs/AlAs SL's coupled via an $Al_yGa_{1-y}As$ spacer layer with $y=0.5$ and variable thickness d_s. Shaded area represents the lowest miniband, while the two lowest interface states (even and odd) are given by solid lines. For comparison, the energy position of a surface state appearing in the corresponding semi-infinite SL is indicated by a full dot. Inset: squared wave function of an interface state for $d_s=120$ Å (solid line) and the respective potential profile (broken line).

the imaginary part μ of the Bloch wave number satisfies the corresponding Kronig-Penney-like dispersion relation, namely,[11]

$$(-1)^n\cosh(\mu d)=\cos(k_a a)\cosh(k_b b) + \tfrac{1}{2}(K^{-1}-K)\sin(k_a a)\sinh(k_b b), \tag{3}$$

where $n=0,1,2,\ldots$ numbers the subsequent SL minigaps.

Inside the spacer layer $(-d_s<z<0)$ the wave function has the following form:

$$\Psi_s(z)=A_2\sinh(k_s z)+A_3\cosh(k_s z), \tag{4}$$

where $k_s=[2m_s(V_s-E)]^{1/2}$, while A_2 and A_3 are determined from the matching of $\Psi_s(z)$ to $\Psi_{sl}(z)$ [given by Eq. (1)] at $z=0$, and read

$$A_2=A_1G, \quad A_3=A_1\lambda, \tag{5}$$

with $G=(k_a m_s)/(k_s m_a)$.

The symmetry property of the considered structure (cf. Fig. 1) implies

$$\Psi_s'\left(-\frac{d_s}{2}\right)=0 \tag{6}$$

for even states and

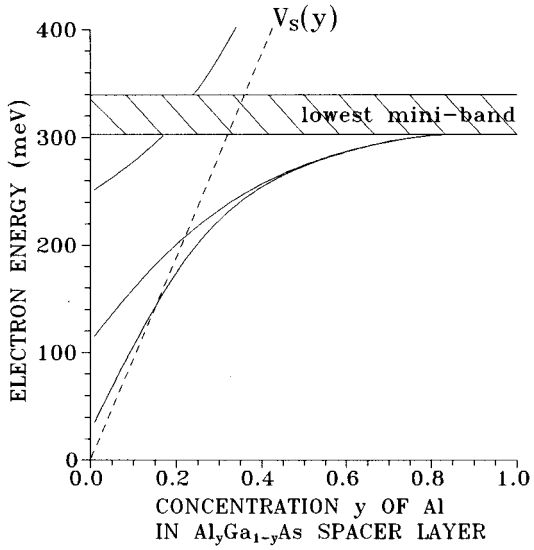

FIG. 3. Electronic structure of GaAs/AlAs SL's coupled via an $Al_yGa_{1-y}As$ spacer layer with $d_s=80$ Å and variable y. Shaded area represents the lowest miniband, while the interface states are given by solid lines. Broken line denotes the spacer-barrier potential height $V_s(y)$.

$$\Psi_s\left(-\frac{d_s}{2}\right)=0 \tag{7}$$

for odd states.

Imposing Eqs. (6) or (7) on Eq. (4) yields the following energy expression:

$$\frac{\lambda}{G}\tanh\left(\frac{k_s d_s}{2}\right)=1 \tag{8}$$

or

$$\frac{\lambda}{G}\coth\left(\frac{k_s d_s}{2}\right)=1 \tag{9}$$

for even and odd localized states, respectively.

The local density of states ρ is calculated using the factorization and direct methods within a framework of the Green function formalism (see, e.g., Ref. 12). The corresponding expression at any arbitrary point z_0 reads[13]

$$\rho(z_0;E)=-\frac{1}{\pi}\mathrm{Im}\mathcal{G}(z_0,z_0;E) =-\frac{2}{\pi}\mathrm{Im}\left[\frac{\Psi_+'(z_0+;E)}{m(z_0+)\Psi_+(z_0;E)} -\frac{\Psi_-'(z_0-;E)}{m(z_0-)\Psi_-(z_0;E)}\right]^{-1}. \tag{10}$$

Here, $\mathcal{G}$ is the Green function of the whole system, whereas $\Psi_+(z;E)$ and $\Psi_-(z;E)$ are the linearly independent solutions to the Schrödinger equation for the energy E which satisfy the given one-sided boundary conditions (outgoing propagation or exponential evanescence) at $z\to+\infty$ and $z\to-\infty$, respectively. In Eq. (1), $\Psi_\pm'(z_0\pm;E)$ and

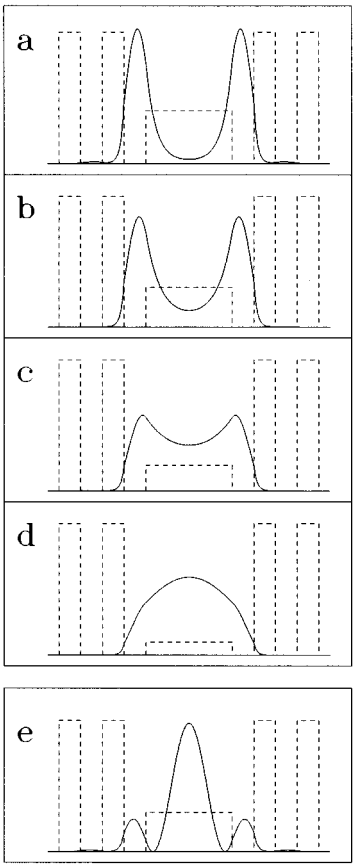

FIG. 4. Squared wave functions (solid lines) of the lowest (a–d) and highest (e) interface states of Fig. 3 for different concentration y of Al in an $Al_yGa_{1-y}As$ spacer layer: (a) $y=0.4$ ($E_{int}=254.24$ meV; $V_s=377.6$ meV), (b) $y=0.3$ ($E_{int}=223.55$ meV; $V_s=283.2$ meV), (c) $y=0.2$ ($E_{int}=174.30$ meV; $V_s=188.8$ meV), (d) $y=0.1$ ($E_{int}=106.17$ meV; $V_s=94.4$ meV), and (e) $y=0.3$ ($E_{int}=374.57$ meV; $V_s=283.2$ meV). Corresponding potential profiles are also presented (broken lines).

$m(z_0\pm)$ denote the right- and left-hand-side limits at z_0 of the derivative of $\Psi_\pm$ and the effective mass m, correspondingly.

Since for E from the SL minigap regions, the density of states is zero except for the discrete energies of localized states, where $\mathcal{G}$ has poles giving rise to δ peaks in the spectrum, only the distributions within the SL miniband regions are of interest, as the density of states is finite there.

In this work, the logarithmic derivative of Ψ_+ (Ψ_-) at z_0 in Eq. (10) is evaluated, for E from the SL miniband regions, by multiple matching of the Schrödinger equation solution for the layer containing z_0 to those for the right-hand-side (left-hand-side) layers, with a final matching [at the right-hand-side (left-hand-side) SL section] to the SL Bloch wave function traveling towards $+\infty$ ($-\infty$). The correct assignment of Ψ_+ and Ψ_- to the respective SL Bloch functions in each miniband is based on the group velocity of an electron.

Equation (10) enables one to calculate the local density of states ρ as a function of energy for a given point z_0 as well as a function of space coordinate for a given energy level E, i.e., the space-charge distributions. The layer density of states can also be computed by integrating ρ over the region under consideration.

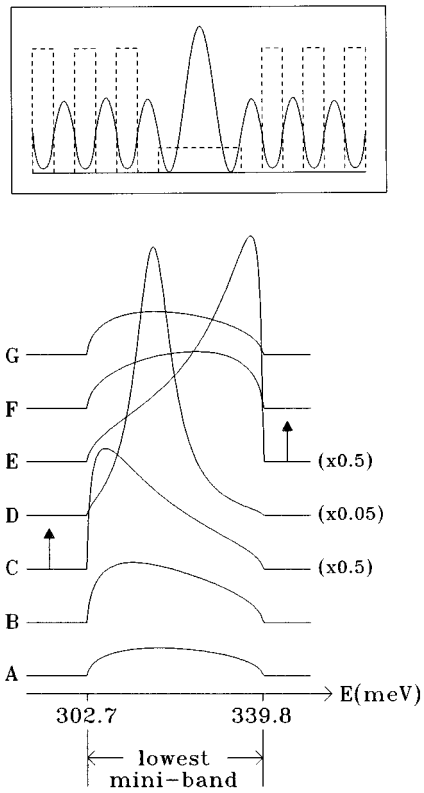

FIG. 5. Layer density-of-states distributions inside the lowest miniband for GaAs/AlAs SL's coupled via an $Al_yGa_{1-y}As$ spacer layer with $d_s=80$ Å and diferent values of y: $y=0$ (curve A), $y=0.1$ (curve B), $y=0.15$ (curve C), $y=0.2$ (curve D), $y=0.25$ (curve E), $y=0.3$ (curve F), and $y=0.4$ (curve G). Arrows denote a position of the highest interface state of Fig. 3 in the proximity of the miniband edges. Inset: space-charge distribution of an interface resonance with the energy corresponding to the maximum of curve D (solid line) as well as the respective potential profile (broken line).

RESULTS

Numerical computations have been performed for SL's made of GaAs and AlAs with the following fixed parameters (cf. Fig. 1): $a=b=20$ Å, $m_a=0.067$, $m_b=0.15$ (note that all the effective masses are given in units of a free-electron mass), and $V_b=944$ meV. The SL's are coupled via an $Al_yGa_{1-y}As$ spacer layer of different thicknesses d_s and variable y, resulting in $V_s=V_s(y)=944y$ meV and $m_s=m_s(y)=0.067+0.083y$.[14] The electronic structure and the density of states of such a system of coupled SL's has been calculated for energies around the lowest miniband as it is the range of most experimental interest.

Localized states

It is natural to expect that when the spacer-barrier layer is thick and high enough, the left- and right-hand-side SL's do not influence each other: they are decoupled and, thus, behave as two independent semi-infinite SL's terminated by a potential barrier $V_s<V_b$. Indeed, as can be seen in Fig. 2, in the lowest minigap there exist a (doubly) degenerate state with the wave function (see the inset of Fig. 2) localized at the outermost quantum well of each of the SL's. Certainly,

its energy coincides with that of a Tamm-like surface state in a corresponding semi-infinite SL (see, e.g., Ref. 10). When the thickness of the spacer-barrier layer decreases, the SL's become really coupled which causes the degenerate state to split into two: even and odd, and we are dealing then with interface rather than surface states.

Figure 3 shows the behavior of the interface states when the spacer-barrier layer has a fixed width $d_s = 80$ Å but variable height $V_s = V_s(y)$. As expected, the energy splitting of the lowest states increases with the decrease of the spacer-barrier height. For y small enough, another interface state appears in the vicinity of the lowest miniband and its energy is always above the spacer-barrier potential $V_s(y)$.

It is interesting to examine, with the help of the corresponding wave functions, the change of the localization properties of the interface states when the spacer-barrier potential is varied. For clarity, and without any loss of generality, we restrict our considerations to the lowest (even) state, as shown in Fig. 4. When the spacer barrier is still quite high ($y = 0.4$), SL's are weakly coupled and the wave function exhibits two distinct maxima in the outermost SL wells and takes very small values inside the spacer region [Fig. 4(a)]. As the potential of the spacer barrier decreases, the maximum-to-minimum difference becomes smaller and smaller [Figs. 4(b) and 4(c)] until one pronounced maximum is reached [Fig. 4(d)] for $y = 0.1$, when the lowest interface state energy E_{int} is already higher than the spacer-barrier potential V_s. Physically this means that an electron with such an energy is localized in the whole region between the two SL's. It is reminiscent of an above-barrier localized state—in fact, whenever the energy E_{int} of any interface state is higher than V_s, we are dealing then with an above-barrier localized state. As an example, the squared wave function of the highest interface state of Fig. 3 is plotted in Fig. 4(e).

Density of states

Density-of-states computations have been performed in order to follow the distribution of extended states inside the lowest miniband. The most pronounced modifications of the density of states are expected around such values of y for which an interface (above-barrier localized) state crosses the miniband (cf. Fig. 3). This particular case is explored in more detail in Fig. 5 via the layer density-of-states distributions, i.e., the local density of states integrated over the spacer layer. For $y = 0$ and $y = 0.4$, when the interface state is well separated from the miniband edges, the layer density-of-states curves exhibit a shape typical for a semi-infinite periodic structure (cf. curves A and G). However, for $y = 0.15$ and $y = 0.25$, when the interface state comes closer to the miniband edges, the layer density-of-states distributions show a pronounced maximum lying close to the appropriate miniband edge (cf. curves C and E). Finally, for $y = 0.2$, when the interface state merges into the miniband, the density-of-states distribution exhibits a sharp and very strong peak (cf. curve D—please note the different scale). The space-charge distribution corresponding to this peak maximum (see the inset of Fig. 5) indicates clearly that we are dealing with a well-defined interface resonance, whose existence—to our best knowledge—has not been demonstrated before.

SUMMARY

In this paper, we have presented theoretical investigations of the electronic structure of GaAs/AlAs SL's coupled via an $Al_yGa_{1-y}As$ spacer layer. Using a direct matching procedure within an envelope-function approximation we have derived expressions for the energy as well as the corresponding wave function of localized electronic states appearing inside the minigaps. This enabled us to follow the transformation from a Tamm-like interface state to an above-barrier localized state.

In addition, the density-of-states distributions inside the minibands have been studied and their modifications due to the change of spacer-layer parameters have been examined. In particular, a possibility of the existence of a well-defined interface resonance in the lowest miniband has been pointed out to be an interesting result.

ACKNOWLEDGMENT

This work has been supported by the University of Wrocław within the Grant No. 2016/W/IFD/96.

[1] G. Lenz and J. Salzman, Appl. Phys. Lett. **56**, 871 (1990).
[2] M. Zahler, I. Brener, G. Lenz, J. Salzman, E. Cohen, and L. Pfeiffer, Appl. Phys. Lett. **61**, 949 (1992).
[3] G. Ihm, S.K. Noh, M.L. Falk, and K.Y. Lim, J. Appl. Phys. **72**, 5325 (1992).
[4] M.-R. Shen, W.-Z. Shen, and Z.-Y. Li, Phys. Status Solidi B **177**, K71 (1993).
[5] M. Zahler, E. Cohen, J. Salzman, E. Linder, and L.N. Pfeiffer, Phys. Rev. Lett. **71**, 420 (1993).
[6] M. Zahler, E. Cohen, J. Salzman, E. Linder, E. Maayar, and L.N. Pfeiffer, Phys. Rev. B **50**, 5305 (1994).
[7] M.R. Vladimirova and A.V. Kavokin, Phys. Solid State **37**, 1178 (1995).
[8] A.V. Kavokin, M.R. Vladimirova, R.P. Seisyan, S.I. Kokhanovskii, M.E. Sasin, V.M. Ustinov, A.Yu. Egorov, and A.E. Zhukov, in *Semiconductor Heteroepitaxy Growth, Characterization and Device Applications*, edited by B. Gil and R.-L. Aulombard (World Scientific, Singapore, 1995), p. 482.
[9] P. Masri, Surf. Sci. Rep. **19**, 1 (1993).
[10] M. Stęślicka, Prog. Surf. Sci. **50**, 65 (1995).
[11] M. Stęślicka, R. Kucharczyk, and M.L. Glasser, Phys. Rev. B **42**, 1458 (1990); M. Stęślicka, R. Kucharczyk, L. Dobrzynski, B. Djafari-Rouhani, E.-H. El Boudouti, and W. Jaskólski, Prog. Surf. Sci. **46**, 219 (1994).
[12] S.G. Davison and M. Stęślicka, *Basic Theory of Surface States* (Clarendon Press, Oxford, 1992).
[13] R. Kucharczyk and M. Stęślicka, Solid State Commun. **84**, 727 (1992).
[14] H. Ohno, E.E. Mendez, J.A. Brum, J.M. Hong, F. Agulló-Rueda, L.L. Chang, and L. Esaki, Phys. Rev. Lett. **64**, 2555 (1990).